2021 18th International Conference on Electrical Engineering, Computing Science and Automatic Control (CCE)
Mexico City, Mexico. November 10-12, 2021

A Novel Method to Analyze Input-Output Controllability

Muhammad Ibrahim
Department of Electrical Engineering
University of Engineering and Technology
Lahore, Faisalabad Campus, Pakistan
ibrahim@uet.edu.pk

Imran Hameed
Department of Mechanical Engineering
The Hong Kong Polytechnic University
Hung Hom, Hong Kong
imran.hameed@connect.polyu.hk

***Abstract*—The proposed algorithm in this research paper leads to an approach through which the input-output controllability of a plant model can be predicted successfully beforehand if it is scaled efficiently according to a normalized behavior. In the industrial applications, it is extremely important to make sure that the inputs and outputs of a plant model are realizable not only with the limitations imposed mostly by the system's devices but also by its circuitry and programming. The motivation behind choosing this method is that the classical control fails to precisely assess the systems. The goal is to extract a threshold value based on the controllability Gramian characteristic. According to a defined controllability criterion, any value which would be less than the proposed threshold value would translate into the fact that the plant is not practically controllable. The Glover-McFarlane loop shaping technique is implemented for a multitude of multi-input multi-output systems.**

***Index Terms*—input-output controllability, $\mathcal{H}_\infty$ controller, scaling, controllability Gramian, multivariable control, MIMO**

I. Introduction

Input-output controllability, also known as performance targeting, is the ability to attain desirable control performance. This is made possible by constraining the magnitudes of the responses $\boldsymbol{y}$ despite having uncertainties within the process parameters or external disturbances $\boldsymbol{d}$, through the use of both measurements ($\boldsymbol{y}_\mathrm{m}$ or $\boldsymbol{d}_\mathrm{m}$) and inputs $\boldsymbol{u}$ [1]. A system is said to be input-output controllable, if it is possible to design a controller that not only rejects the disturbances but also tracks the reference signals [2].

The idea of controllability in control systems theory helps us to analyze control performance efficiently. Previous work investigates the controllability of single input single output control systems as well as networked structures. In [3], loop shaping technique is used to perform the input-output controllability analysis on time delayed SISO plant models, featuring the properties of disturbance rejection and command tracking. The controllability methods for the open loop analysis under the constraints are explained in [4]. Recent publications discussing the concepts, approaches and applications of controllability in biological and large-scale networks are presented in [5]–[7].

With the realization of advanced and state-of-the-art complex systems, the methods of controllability demand a continuous improvement. The classical control theory cannot precisely predict the controllability of the systems beforehand and researchers always keen to improve existing methods or develop new techniques. This work is a step in this direction. The plant models, if analyzed rigorously, can be judged for their behavior before the design of an optimal controller. Such methods play a key role in control systems theory and prove to be handy for engineers to ascertain the performance of a system before it is practically implemented [8], [9].

Section II presents the mathematical preliminaries. The Glover-McFarlane $\mathcal{H}_\infty$ controller design is discussed in section III. The proposed controllability analysis of a multitude of the multi-input multi-output unstable plant models with zeros in the right half plane is examined in section IV. Finally, conclusions are drawn in section V.

II. Mathematical Preliminaries

A. Controllability Gramian

If the Gramian matrix $\boldsymbol{W}_\mathrm{c}(t)$ possesses a full rank for a time $t > 0$, then the linear system $(\boldsymbol{A}, \boldsymbol{B})$ is considered to be controllable [10]. The controllability Gramian of a system $(\boldsymbol{A}, \boldsymbol{B})$ is given by [11] as,

$$\boldsymbol{W}_\mathrm{c}(t) = \int_0^t e^{\boldsymbol{A}\tau} \boldsymbol{B}\boldsymbol{B}^\mathrm{T} e^{\boldsymbol{A}^\mathrm{T}\tau} d\tau \tag{1}$$

The elements of the controllability Gramian matrix are relatively of the same order of magnitude which results in the evaluation of its rank much reliable in comparison to the Kalman and Gilbert controllability matrices. The controllability Gramian can also be derived as a solution to the Lyapunov equation [12] as,

$$\boldsymbol{A}\boldsymbol{W}_\mathrm{c}(t) + \boldsymbol{W}_\mathrm{c}(t)\boldsymbol{A}^\mathrm{T} = -\boldsymbol{B}\boldsymbol{B}^\mathrm{T} \tag{2}$$

The controllability Gramian defined by (1) cannot be extended to unstable systems since the integrals will become unbounded [13]. The MATLAB® command `gram` has a prerequisite condition that the system matrix $\boldsymbol{A}$ must be stable. In order to determine the controllability Gramian for an unstable system $(\boldsymbol{A}, \boldsymbol{B})$, the function given by [14] is utilized. The system matrix $\boldsymbol{A}$ is decomposed by using the Schur decomposition [15]. The Lyapunov equations are then solved to decouple the system into stable and unstable parts respectively. The transformation $\boldsymbol{T}_\mathrm{r}$ is obtained from the resulting decoupled

978-1-6654-0029-9/21/$31.00 ©2021 IEEE

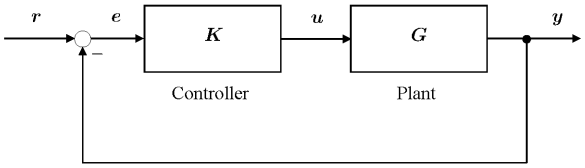

Fig. 1. One degree of freedom control configuration

system. In the end, Cholesky factorization is done to compute the controllability Gramian in the state space form for an unstable system [16].

In Fig. 1, the closed loop response $\boldsymbol{y}$ can be defined as a function of the complementary sensitivity function $\boldsymbol{T}$ as,

$$\boldsymbol{y} = \boldsymbol{T}\boldsymbol{r} \tag{3}$$

where $\boldsymbol{T}$ can be represented in terms of the plant $\boldsymbol{G}$ and controller $\boldsymbol{K}$ as,

$$\boldsymbol{T} = (\boldsymbol{I} + \boldsymbol{G}\boldsymbol{K})^{-1}\boldsymbol{G}\boldsymbol{K} = (\boldsymbol{I} + \boldsymbol{L})^{-1}\boldsymbol{L} \tag{4}$$

and $\boldsymbol{L} = \boldsymbol{G}\boldsymbol{K}$ is the open loop transfer function. In Fig. 1, the control error $\boldsymbol{e}$ is given as,

$$\boldsymbol{e} = \boldsymbol{S}\boldsymbol{r} = (\boldsymbol{I} + \boldsymbol{G}\boldsymbol{K})^{-1}\boldsymbol{r} = (\boldsymbol{I} + \boldsymbol{L})^{-1}\boldsymbol{r} \tag{5}$$

where $\boldsymbol{S}$ represents the sensitivity function.

The sensitivity function $\boldsymbol{S}$ is an important indicator of the closed loop performance. The performance will be improved by reducing $|\boldsymbol{e}|$ at all frequencies. Here, the word "performance" specifies the smallness of the sensitivity function $\boldsymbol{S}$.

Now the input signal $\boldsymbol{u}$ to the plant $\boldsymbol{G}$ is given as,

$$\boldsymbol{u} = \boldsymbol{K}\boldsymbol{S}\boldsymbol{r} \tag{6}$$

Equation (6) suggests that it is required to keep the norm of the closed loop transfer function $\boldsymbol{K}\boldsymbol{S}$ small in order to limit the magnitude of the input signal for reference tracking.

B. Scaling

Scaling of a control process plays a decisive role in the input-output controllability analysis. The peaks of the closed loop transfer functions ($\boldsymbol{S}$, $\boldsymbol{T}$ or $\boldsymbol{K}\boldsymbol{S}$) depend on the scaling of the control variables. These scaled plants can then be compared quantitatively to find a common characteristic threshold. The scaling is achieved by limiting the magnitude of the variables within the bounds of ± 1 [17]. By following this approach, the input-output controllability of a plant model can be predicted successfully beforehand if they are scaled according to some normalized behavior.

Considering the output of a plant in terms of the transfer function and the control input as,

$$\acute{\boldsymbol{y}} = \acute{\boldsymbol{G}}\acute{\boldsymbol{u}} \tag{7}$$

The unscaled variables are represented by the sign ($\acute{}$). The error signal, defined as the difference between the reference signal and response, is obtained as,

$$\acute{\boldsymbol{e}} = \acute{\boldsymbol{r}} - \acute{\boldsymbol{y}} \tag{8}$$

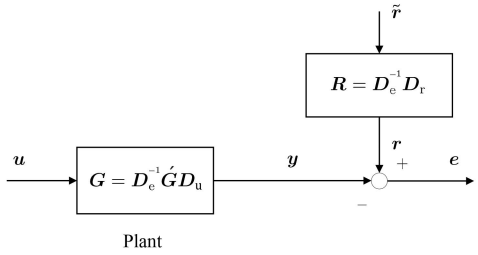

Fig. 2. Scaled plant model

The aim of a control process is to limit the error i. e. $|\boldsymbol{e}| < 1$. In order to accomplish this goal, it is required to scale the input variable with respect to the maximum control input and the other variables (error and output) relative to the allowed control error i. e.

$$\boldsymbol{u} = \boldsymbol{D}_{\mathrm{u}}^{-1}\acute{\boldsymbol{u}}, \;\; \boldsymbol{e} = \boldsymbol{D}_{\mathrm{e}}^{-1}\acute{\boldsymbol{e}}, \;\; \boldsymbol{y} = \boldsymbol{D}_{\mathrm{e}}^{-1}\acute{\boldsymbol{y}} \tag{9}$$

where the scaling matrices $\boldsymbol{D}_{\mathrm{u}}$ and $\boldsymbol{D}_{\mathrm{e}}$ are given as,

$$\boldsymbol{D}_{\mathrm{u}} = \mathrm{diag}(\acute{\boldsymbol{u}}_{\max}), \;\; \boldsymbol{D}_{\mathrm{e}} = \mathrm{diag}(\acute{\boldsymbol{e}}_{\max}) \tag{10}$$

Inserting (7) into (9) gives the output signal $\boldsymbol{y}$ as,

$$\boldsymbol{y} = \boldsymbol{D}_{\mathrm{e}}^{-1}\acute{\boldsymbol{G}}\acute{\boldsymbol{u}} \tag{11}$$

Now by substituting the unscaled input signal $\acute{\boldsymbol{u}}$ from (9) results in the following scaled plant output as,

$$\boldsymbol{y} = \boldsymbol{D}_{\mathrm{e}}^{-1}\acute{\boldsymbol{G}}\boldsymbol{D}_{\mathrm{u}}\boldsymbol{u} \tag{12}$$

or

$$\boldsymbol{y} = \boldsymbol{G}\boldsymbol{u} \tag{13}$$

where the magnitudes of both the output and input signals are required to be $|\boldsymbol{y}| < 1$ and $|\boldsymbol{u}| < 1$ respectively [18].

The reference signal is also scaled by the introduction of a scaling block $\boldsymbol{R}$. From Fig. 2, the reference signal $\boldsymbol{r}$ is given as,

$$\boldsymbol{r} = \boldsymbol{R}\tilde{\boldsymbol{r}} = \boldsymbol{D}_{\mathrm{e}}^{-1}\boldsymbol{D}_{\mathrm{r}}\tilde{\boldsymbol{r}} \tag{14}$$

where $\boldsymbol{D}_{\mathrm{r}} = \mathrm{diag}(\acute{\boldsymbol{r}}_{\max})$ represents the scaling matrix.

If the controllability is changed by scaling, the plant is effectively re-scaled to another one. Scaling simply means changing the maximum possible actuation and the maximum allowed control error. So in fact, to make an uncontrollable plant, controllable by scaling, the plant is reconfigured to have a more expensive, bigger actuator and/or the requirement for the error tolerance is lessened [19], [20].

III. $\mathcal{H}_\infty$ Controller Design

The Glover-McFarlane loop shaping technique is implemented for a multitude of multi-input multi-output MIMO systems. In this method, a controller is synthesized by minimizing an $\mathcal{H}_\infty$ performance objective [21]. The closed loop transfer functions are shaped by the selection of the appropriate weights in order to limit the magnitudes of the input and output signals respectively [22]. The $\mathcal{H}_\infty$ optimal controller is obtained for which the ∞-norm of the stacked

matrix $\boldsymbol{N}$, based on the 'mixed sensitivity' specifications, is minimized [23].

$$\boldsymbol{N} = \begin{bmatrix} \boldsymbol{W}_{\mathrm{p}}\boldsymbol{S} \\ \boldsymbol{W}_{\mathrm{u}}\boldsymbol{K}\boldsymbol{S} \end{bmatrix} \tag{15}$$

The control objective is to minimize,

$$\gamma_{\min} = \min_{\mathbf{K}} ||\boldsymbol{N}(\boldsymbol{K})||_{\infty} \tag{16}$$

The variable $\gamma_{\min}$ is the $\mathcal{H}_{\infty}$ norm of the closed loop transfer functions ($\boldsymbol{S}$ and $\boldsymbol{K}\boldsymbol{S}$) that can be tolerated before the instability is reached. The measure $\gamma_{\min}$ is needed to be small as much as possible in order to achieve a better performance [24].

A. Performance weight $\boldsymbol{W}_{\mathrm{p}}$

The weight, $\boldsymbol{W}_{\mathrm{p}} = \mathrm{diag}(w_{\mathrm{p}_i})$, associated with the sensitivity function $\boldsymbol{S}$ is regarded as the performance weight. It amplifies the sensitivity function $\boldsymbol{S}$ at low frequencies, giving them more significance. Roughly, it is an integrator.

$$w_{\mathrm{p}_i} = \frac{s/M_i + \omega^{\star}_{\mathrm{B}_i}}{s + \omega^{\star}_{\mathrm{B}_i} A_i} \tag{17}$$

where $\omega^{\star}_{\mathrm{B}_i}$ is the desired closed loop bandwidth. The subscript i refers to the corresponding channel. However, the subscript is omitted in Fig. 3 and in the formulas for the sake of simplification.

The performance weight w_{p} is used to put a bound on the sensitivity function $\boldsymbol{S}$, so it requires that,

$$||w_{\mathrm{p}}\boldsymbol{S}||_{\infty} < 1 \quad \forall \boldsymbol{\omega} \tag{18}$$

The above condition states that the ∞-norm of the product of the performance weight w_{p} and the sensitivity function $\boldsymbol{S}$ should be less than 1 for all frequencies [25]. But practically, with a given controller, the weighted sensitivity exceeds 1 at some frequencies due to the presence of the RHP zeros and RHP poles.

At low frequencies, it can be observed from Fig. 3 that the inverse of the performance weight $|1/w_{\mathrm{p}}|$ is equal to A. At high frequencies, it becomes equal to M which is greater than 1. The asymptote shown by the dotted line crosses the magnitude of 1, at the frequency $\omega^{\star}_{\mathrm{B}}$, which is approximately the bandwidth requirement [26].

1) Limitations imposed by the right half plane (RHP) zero: The presence of the RHP zero shows an inverse response in the output of a control system which limits the response speed. It is therefore, necessary to consider these limitations to avoid the instabilities. Consider a plant model having the RHP zero at $s = z_{\mathrm{RHP}}$, then it is required for the performance weight (17) to satisfy the condition given in (18) as,

$$|w_{\mathrm{p}}(z_{\mathrm{RHP}})| = \left| \frac{z_{\mathrm{RHP}}/M + \omega^{\star}_{\mathrm{B}}}{z_{\mathrm{RHP}} + \omega^{\star}_{\mathrm{B}} A} \right| < 1 \tag{19}$$

The bound on the achievable bandwidth can then be derived as follows,

$$\omega^{\star}_{\mathrm{B}} < z_{\mathrm{RHP}} \frac{1 - 1/M}{1 - A} \tag{20}$$

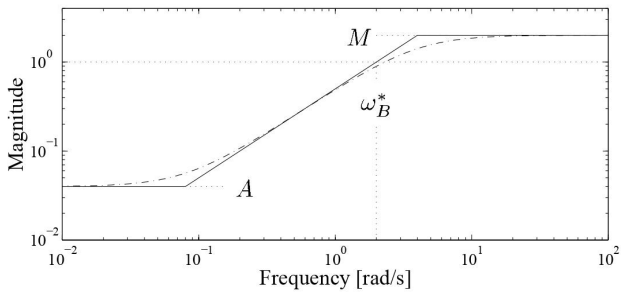

Fig. 3. Inverse of the performance weight $|1/w_{\mathrm{p}}|$

The limitation imposed by the right half plane zero can be derived if M is selected as 2 and $A = 0$. Referring back to (17) and (18), these specifications give a minimum weight of $1/2$ at high frequencies (instead of a pure integrator without s/M), resulting in the sensitivity function of less than 2 for all frequencies [27]. Finally, a limitation on the bandwidth is derived as,

$$\omega^{\star}_{\mathrm{B}} < z_{\mathrm{RHP}}/2 \tag{21}$$

2) Limitations imposed by the right half plane (RHP) pole: For the case of a right half plane pole, the bandwidth $\omega^{\star}_{\mathrm{B}}$ should be greater than two times of the pole frequency. Large feedback gains are usually required to stabilize an unstable plant [28]. The limitation which is imposed by the RHP pole, is recommended by Åström [29] as,

$$\omega^{\star}_{\mathrm{B}} > 2p_{\mathrm{RHP}} \tag{22}$$

If a plant contains both the right half plane zero and pole respectively, then the combination of the conditions, given by (21) and (22), results in,

$$2p_{\mathrm{RHP}} < \omega^{\star}_{\mathrm{B}} < z_{\mathrm{RHP}}/2 \tag{23}$$

The above condition provides an interesting relation among the RHP zero and the RHP pole, which suggests that they should be well separated.

$$z_{\mathrm{RHP}} > 4p_{\mathrm{RHP}} \tag{24}$$

B. Input weight $\boldsymbol{W}_{\mathrm{u}}$

The weight, $\boldsymbol{W}_{\mathrm{u}} = \mathrm{diag}(w_{\mathrm{u}_i})$, deals with the input signal $\boldsymbol{u}$. From (6), the product of $\boldsymbol{K}\boldsymbol{S}$ represents the closed loop transfer function from the reference $\boldsymbol{r}$ to the control input $\boldsymbol{u}$.

The weight $\boldsymbol{W}_{\mathrm{u}}$ is usually a high pass filter, because the actuator cannot handle high frequencies well or its wear is increased which results in the saturation of the input signal $\boldsymbol{u}$ [30]. Therefore, it is recommended to use a filter of the form,

$$w_{\mathrm{u}_i} = \frac{s}{s + \omega_i} \tag{25}$$

where ω_i is approximately the closed loop bandwidth of the corresponding channel.

The controllability is determined based on the criterion that if the output signal $\boldsymbol{y}$, error signal $\boldsymbol{e}$ and input signal $\boldsymbol{u}$

TABLE I
CONTROLLABILITY CRITERIA

Controllability	Proposed Criterion
Controllable	$[\lvert \boldsymbol{e}_{\text{peak}} \rvert \wedge \lvert \boldsymbol{u}_{\text{peak}} \rvert \wedge \lvert \boldsymbol{y}_{\text{peak}} \rvert] < 1$
Uncontrollable	$[\lvert \boldsymbol{e}_{\text{peak}} \rvert \vee \lvert \boldsymbol{u}_{\text{peak}} \rvert \vee \lvert \boldsymbol{y}_{\text{peak}} \rvert] \geq 1$

altogether have peak amplitudes less than 1, then it corresponds that the plant is practically input-output controllable. On the contrary, the plants for which $|\boldsymbol{u}|$, $|\boldsymbol{e}|$ or $|\boldsymbol{y}|$ exceed the magnitude of 1, indicate that the plant is practically uncontrollable. The proposed controllability criteria is given by Table I. The symbol $\vee$ represents the logical OR operator and $\wedge$ represents the logical AND operator.

IV. INPUT-OUTPUT CONTROLLABILITY ANALYSIS OF RANDOM MULTI-INPUT MULTI-OUTPUT PLANTS

The goal is to obtain a common threshold value based on the controllability Gramian characteristic represented by w_{c} for a wide number of multi-input multi-output systems. The scaling of each plant model has been performed by dividing each plant output by the maximum expected control error $\acute{e}_{\max}$. The plant model is given as a combination of two subsystems $\boldsymbol{N}_{\text{p}}$ and $\boldsymbol{N}_{\text{z}}$ respectively based on all the levels of the interactions i. e. rotation matrix $\boldsymbol{R}_{\alpha}$.

$$\boldsymbol{G} = \underbrace{\begin{bmatrix} \frac{1}{s-p_{\text{RHP}}} & 0 \\ 0 & \frac{1}{s+3} \end{bmatrix}}_{\boldsymbol{N}_{\text{p}}} \underbrace{\begin{bmatrix} \cos\alpha & -\sin\alpha \\ \sin\alpha & \cos\alpha \end{bmatrix}}_{\boldsymbol{R}_{\alpha}} \underbrace{\begin{bmatrix} \frac{s-z_{\text{RHP}}}{0.1s+1} & 0 \\ 0 & \frac{s+2}{0.1s+1} \end{bmatrix}}_{\boldsymbol{N}_{\text{z}}}$$

where the matrix $\boldsymbol{N}_{\text{p}}$ contains the RHP pole and the matrix $\boldsymbol{N}_{\text{z}}$ comprises of the RHP zero.

The plant $\boldsymbol{G}$ contains four poles among which two poles are located at $p_1 = p_2 = -10$ and the third one is at $p_3 = -3$. It has two zeros; one of them is at $z_1 = -2$. The directions of both poles and zeros affect the input-output controllability. The bandwidth of the corresponding channel, for the selection of the weights and other parameters, is varied according to the conditions that were stated in the previous section. The angle α is divided into 16 intervals ranging from $0°$ to $90°$ with a step size of $6°$ apart. For $\alpha = 0°$, it can be observed that the rotation matrix $\boldsymbol{R}_{\alpha}$ will become an identity matrix $\boldsymbol{I}$ and the plant model $\boldsymbol{G}$ will be comprised of two decoupled subsystems. For the intermediate directions, there will always be some sort of an interaction. Again, at $\alpha = 90°$, the plant will be comprised of two decoupled subsystems. The range for the Gramian based controllability characteristic will be presented along with the angles of α, ranging from $0°$ to $90°$, in a tabular form as well as in the graphical illustration.

A. Random systems based on a variable RHP pole

The position of the right half plane pole p_{RHP} is changed initially and afterwards, the position of the RHP zero is varied. The RHP pole ranges from $p_{\text{RHP}} = 0.4$ to $p_{\text{RHP}} = 0.8$. The position of the RHP zero is $z_{\text{RHP}} = 4$. The determinant for the controllability Gramian represented by w_{c1} ranges from 0.116 to 2.405 for all the levels of interactions as it can be observed from case I in Table II.

TABLE II
INPUT-OUTPUT CONTROLLABILITY ANALYSIS OF MULTI-INPUT MULTI-OUTPUT PLANT MODELS WITH A VARIABLE RHP POLE

Case	I	II	III	IV	V
	$p_{\text{RHP}} = 0.4$ $z_{\text{RHP}} = 4$	$p_{\text{RHP}} = 0.5$ $z_{\text{RHP}} = 4$	$p_{\text{RHP}} = 0.6$ $z_{\text{RHP}} = 4$	$p_{\text{RHP}} = 0.7$ $z_{\text{RHP}} = 4$	$p_{\text{RHP}} = 0.8$ $z_{\text{RHP}} = 4$
Alpha α	w_{c1}	w_{c2}	w_{c3}	w_{c4}	w_{c5}
0°	0.116	0.094	0.077	0.065	0.055
6°	0.167	0.124	0.096	0.076	0.062
12°	0.331	0.247	0.191	0.152	0.123
18°	0.584	0.436	0.339	0.271	0.221
24°	0.897	0.673	0.526	0.423	0.348
30°	1.236	0.935	0.737	0.597	0.495
36°	1.569	1.197	0.952	0.78	0.654
42°	1.866	1.439	1.158	0.96	0.814
48°	2.106	1.644	1.34	1.127	0.969
54°	2.278	1.804	1.492	1.273	1.11
60°	2.384	1.918	1.611	1.394	1.234
66°	2.432	1.989	1.696	1.489	1.336
72°	2.44	2.027	1.753	1.56	1.416
78°	2.428	2.043	1.1788	1.607	1.473
84°	2.412	2.048	1.806	1.634	1.507
90°	2.405	2.048	1.811	1.643	1.518

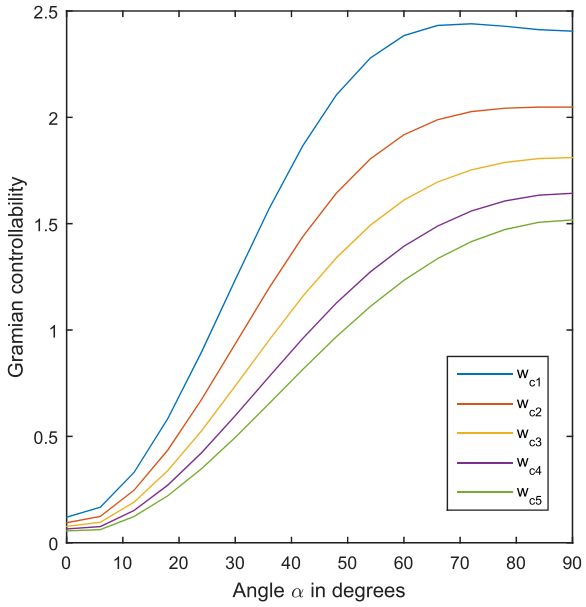

Fig. 4. Controllability Gramian curves with a variable RHP pole

In case II, the RHP pole of the plant $\boldsymbol{G}$ is increased by a summand of 0.1 i. e. $p_{\text{RHP}} = 0.5$, while the position of z_{RHP} is retained. This time, it can be seen that the overall controllability Gramian w_{c2} is decreased as compared to the case I. For case III, again the RHP pole of the plant $\boldsymbol{G}$ is slightly shifted, making it at $p_{\text{RHP}} = 0.6$. The determinant for the controllability Gramian w_{c3} seems to be depreciated again as compared to the preceding case. The same holds for the rest of the cases.

It can be stated that the overall Gramian based controlla-

bility characteristic w_c decreases as the RHP pole is moving towards the right side of the s-plane. It seems plausible because the system is becoming more unstable, and also the unstable pole is getting closer to the RHP zero, thus making it more difficult to control. To summarize this, the farther the roots from the real axis, the more problematic the control will be. This can be observed from Fig. 4 in which Gramian curves show a deteriorating effect as p_{RHP} is shifted towards the right side of the s-plane.

B. Random systems based on a variable RHP zero

Now the position of the right half plane zero z_{RHP} is varied. The first multi-input multi-output system, that is considered, has the RHP pole at $p_{\mathrm{RHP}} = 0.5$ and the position of the RHP zero is $z_{\mathrm{RHP}} = 3.6$. In Table III, case VI shows that the determinant for the controllability Gramian represented by w_{c6} ranges from 0.094 to 1.718 for all the angles of α. By taking a look at the other cases, it can be verified that as the RHP zero is moving towards the right side of the real axis of the s-plane, the Gramian based controllability characteristic w_c seems to be improving. The reason is that the RHP zero and the RHP pole are getting well separated for each case which holds true in accordance with the condition given by (24). Fig. 5 illustrates the controllability Gramian curves graphically for these systems having a variable RHP zero along with the angles of α on the basis of all the levels of interactions.

C. Deriving the threshold value of the controllability Gramian

The magnitudes of all the input, error, and output signals were assessed. Although their magnitudes are not presented here, however, all these values were exported to the Microsoft Excel spreadsheet files, before and after the normalization. Each plant model is scaled by a factor of $\boldsymbol{D}_{\mathrm{e}} = 1.44 \cdot \boldsymbol{I}$, where $\boldsymbol{I}$ is an identity matrix. The scaling matrix $\boldsymbol{D}_{\mathrm{u}}$ is chosen to be an identity matrix which signifies that the input signals are not scaled even though the peak magnitudes of some input values were out of bounds.

As the location of the poles and zeros is varied, the resultant impact reflected on the controllability Gramian characteristic value are observed. Lastly, a threshold value is deduced which comes out to be $w_{\mathrm{c,thres}} = 1.004$. The values less than this threshold are treated as uncontrollable. According to the set controllability criteria, the controllability Gramian states that each plant model is practically controllable for the value of $w_c \geq 1.004$.

Eventually, all the controllability Gramian curves for these multi-input multi-output MIMO plants (along the x-axis) are shown graphically against the peak magnitudes of the input, error and output signals respectively (along the y-axis) in Fig. 6. The upper left corner represents the uncontrollability region. As the maximum magnitude of one of these signals decreases, the controllability Gramian seems to be improving. Once it slides down to the magnitude of 1, we enter into the region of practical controllability (lower right corner). It can be observed that the intersection of the two dotted lines ultimately provides the threshold of the controllability Gramian characteristic.

TABLE III
INPUT-OUTPUT CONTROLLABILITY ANALYSIS OF MULTI-INPUT MULTI-OUTPUT PLANT MODELS WITH A VARIABLE RHP ZERO

Case	**VI**	**VII**	**VIII**	**IX**	**X**
	$p_{\mathrm{RHP}} = 0.5$ $z_{\mathrm{RHP}} = 3.6$	$p_{\mathrm{RHP}} = 0.5$ $z_{\mathrm{RHP}} = 3.7$	$p_{\mathrm{RHP}} = 0.5$ $z_{\mathrm{RHP}} = 3.8$	$p_{\mathrm{RHP}} = 0.5$ $z_{\mathrm{RHP}} = 3.9$	$p_{\mathrm{RHP}} = 0.5$ $z_{\mathrm{RHP}} = 4$
Alpha α	w_{c6}	w_{c7}	w_{c8}	w_{c9}	w_{c10}
0°	0.094	0.094	0.094	0.094	0.094
6°	0.089	0.097	0.105	0.114	0.124
12°	0.17	0.187	0.205	0.225	0.247
18°	0.297	0.328	0.361	0.397	0.436
24°	0.459	0.507	0.558	0.613	0.673
30°	0.644	0.709	0.778	0.854	0.935
36°	0.837	0.917	1.004	1.097	1.197
42°	1.026	1.118	1.217	1.324	1.439
48°	1.199	1.299	1.406	1.521	1.644
54°	1.35	1.452	1.562	1.679	1.804
60°	1.473	1.574	1.682	1.796	1.918
66°	1.569	1.665	1.767	1.875	1.989
72°	1.638	1.728	1.823	1.923	2.027
78°	1.684	1.768	1.856	1.948	2.043
84°	1.71	1.79	1.873	1.959	2.048
90°	1.718	1.797	1.878	1.962	2.048

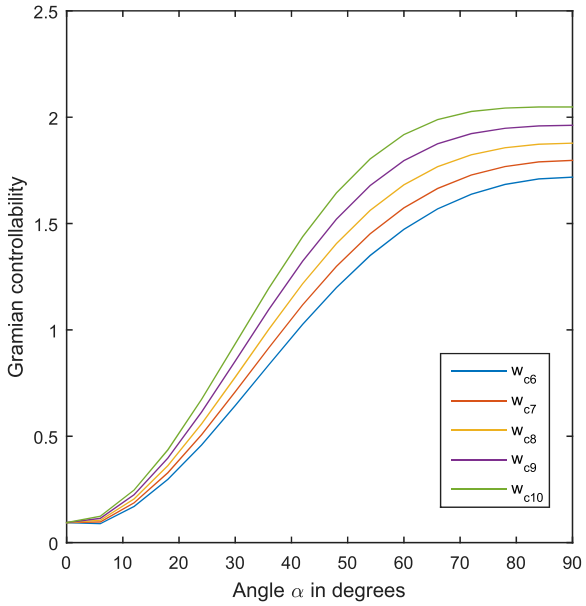

Fig. 5. Controllability Gramian curves with a variable RHP zero

V. CONCLUSION

The role of scaling in any control system is significant. If this scheme is applied to a wide set of scaled systems, signifying the maximum available values and additionally designing an optimal controller by taking into account the system's properties, then it is possible to perform a quantitative evaluation for the controllability matrices. The deduced threshold value of the controllability characteristic is admissible to all the varied versions of the plants assumed in this article. The significance of finding the Gramian characteristic threshold is to precisely predict the input-output controllability. This paper

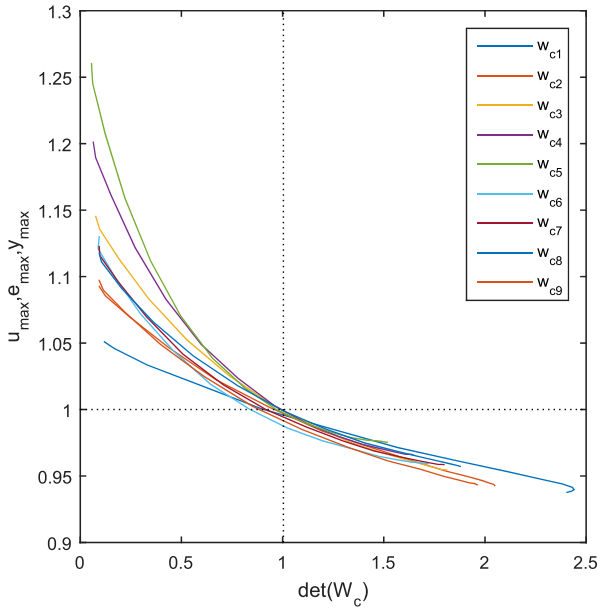

Fig. 6. Controllability Gramian curves along with the peak magnitudes of the input, error and output signals

also encourages quantifying the limits of the variables involved in any control configuration.

Each and every plant shares its own characteristics and limitations i. e. the influence of disturbances, experiencing stability issues, dead time and a reasonable degree of uncertainty (measure of robustness). This paper covers a multitude of unstable MIMO models having a zero in the right half plane. However, the prospects of refining the controllability characteristic look bright to ensure that the threshold value is admissible to every possible industrial control process.

REFERENCES

[1] S. Skogestad, "A procedure for SISO controllability analysis-with application to design of pH neutralization processes," *Computers & chemical engineering*, vol. 20, no. 4, pp. 373–386, 1996.

[2] Y. Li, J. Li, Z. Ma, J.-e. Feng, and H. Wang, "Controllability and observability of state-dependent switched Boolean control networks with input constraints," *Asian Journal of Control*, vol. 21, no. 6, pp. 2662–2673, 2019.

[3] M. Ibrahim and I. Hameed, "Disturbance rejection and reference tracking of time delayed systems using Gramian controllability," *International Journal of Dynamics and Control*, pp. 1–8, 2021.

[4] Y. Cao, D. Biss, and J. Perkins, "Assessment of input-output controllability in the presence of control constraints," *Computers & Chemical Engineering*, vol. 20, no. 4, pp. 337–346, 1996.

[5] Y. Xia, R. Li, M. Yin, and Y. Zou, "A quantitative measure of the degree of output controllability for output regulation control systems: Concept, approach, and applications," *Journal of Vibration and Control*, p. 10775463211020185, 2021.

[6] G. Casadei, C. Canudas-de Wit, and S. Zampieri, "Model reduction based approximation of the output controllability gramian in large-scale networks," *IEEE Transactions on Control of Network Systems*, vol. 7, no. 4, pp. 1778–1788, 2020.

[7] L. Wu, M. Li, J.-X. Wang, and F.-X. Wu, "Controllability and its applications to biological networks," *Journal of Computer Science and Technology*, vol. 34, no. 1, pp. 16–34, 2019.

[8] G. Joseph and C. R. Murthy, "Controllability of Linear Dynamical Systems Under Input Sparsity Constraints," *IEEE Transactions on Automatic Control*, vol. 66, no. 2, pp. 924–931, 2021.

[9] Z. Al-Zhour, "Controllability and observability behaviors of a non-homogeneous conformable fractional dynamical system compatible with some electrical applications," *Alexandria Engineering Journal*, 2021.

[10] G. Baggio, S. Zampieri, and C. W. Scherer, "Gramian optimization with input-power constraints," in *2019 IEEE 58th Conference on Decision and Control (CDC)*, pp. 5686–5691, IEEE, 2019.

[11] W. Rugh, *Linear System Theory*. Prentice-Hall information and system sciences series, Prentice Hall, 2nd ed., 1996.

[12] M. A. Wicks and R. A. DeCarlo, "Gramian assignment based on the Lyapunov equation," *IEEE Transactions on Automatic Control*, vol. 35, pp. 465–468, April 1990.

[13] F. Bengtsson, "Development and evaluation of methods for control and modelling of multiple-input multiple-output systems," 2020.

[14] Chris Bowden, "Controllability gramian for unstable systems." https://www.mathworks.com/matlabcentral/fileexchange/38328-controllability-gramian-for-unstable-systems/, 2021. MATLAB Central File Exchange.

[15] A. Dmytryshyn, "Schur decomposition of several matrices," *arXiv preprint arXiv:2002.04550*, 2020.

[16] M. Rydel and R. Stanisławski, "Computation of controllability and observability Gramians in modeling of discrete-time noncommensurate fractional-order systems," *Asian Journal of Control*, vol. 22, no. 3, pp. 1052–1064, 2020.

[17] K. Łakomy, M. M. Michałek, and W. Adamski, "Scaling of commanded signals in a cascade control system addressing velocity and acceleration limitations of robotic UAVs," *IFAC-PapersOnLine*, vol. 52, no. 12, pp. 73–78, 2019. 21st IFAC Symposium on Automatic Control in Aerospace ACA 2019.

[18] G. Rabatel, F. Marini, B. Walczak, and J.-M. Roger, "VSN: Variable sorting for normalization," *Journal of Chemometrics*, vol. 34, no. 2, p. e3164, 2020.

[19] P. Albertos and I. Mareels, *Feedback and Control for Everyone*. Springer Berlin Heidelberg, 2010.

[20] C. Saunders and N. Shlomo, "A new approach to assess the normalization of differential rates of protest participation," *Quality & Quantity*, pp. 1–24, 2020.

[21] A. A. Peters, F. J. Vargas, and J. Chen, "An Algebraic Formula for Performance Bounds of a Weighted H-infinity Optimal Control Problem," *IEEE Transactions on Automatic Control*, 2020.

[22] A. H. Mhmood and H. I. Ali, "Optimal H-infinity Integral Dynamic State Feedback Model Reference Controller Design for Nonlinear Systems," *Arabian Journal for Science and Engineering*, pp. 1–14, 2021.

[23] P. Saini, K. Charu, and M. Bisht, "Design of Controller for Stock Consistency Control using H-Infinity Mixed Sensitivity Approach," in *2019 International Conference on Innovative Sustainable Computational Technologies (CISCT)*, pp. 1–6, IEEE, 2019.

[24] X. Yan, P. Wang, J. Qing, S. Wu, and F. Zhao, "Robust power control design for a small pressurized water reactor using an H infinity mixed sensitivity method," *Nuclear Engineering and Technology*, vol. 52, no. 7, pp. 1443–1451, 2020.

[25] T. Benjanarasuth, "Simplified controller design for output performance under common input limitations with generalized integral anti-windup for a class of processes," *ASEAN Engineering Journal*, vol. 10, no. 1, pp. 64–78, 2020.

[26] S. Skogestad and I. Postlethwaite, *Multivariable Feedback Control: Analysis and Design*. The Atrium, Southerm Gate, Chichester, West Sussex, England: John Wiley and Sons, Ltd., 2nd ed., 2005.

[27] E. Tegling, P. Mitra, H. Sandberg, and B. Bamieh, "On fundamental limitations of dynamic feedback control in regular large-scale networks," *IEEE Transactions on Automatic Control*, vol. 64, no. 12, pp. 4936–4951, 2019.

[28] C. Onat, "A new design method for PI–PD control of unstable processes with dead time," *ISA transactions*, vol. 84, pp. 69–81, 2019.

[29] K. J. Åström, "Control system design lecture notes for me 155a," *Department of Mechanical and Environmental Engineering University of California Santa Barbara*, vol. 333, 2002.

[30] S. A. Bortoff, P. Schwerdtner, C. Danielson, and S. Di Cairano, "H-Infinity Loop-Shaped Model Predictive Control with Heat Pump Application," in *2019 18th European Control Conference (ECC)*, pp. 2386–2393, IEEE, 2019.